Neurobiology of Disease 71 (2014) 305–316

Contents lists available at ScienceDirect

Neurobiology of Disease

journal homepage: www.elsevier.com/locate/ynbdi

Gabapentin attenuates hyperexcitability in the freeze-lesion model of developmental cortical malformation

Lauren Andresen [a,b], David Hampton [a], Amaro Taylor-Weiner [c,1], Lydie Morel [a], Yongjie Yang [a], Jamie Maguire [a], Chris G. Dulla [a,*]

[a] Department of Neuroscience, Tufts University School of Medicine, 136 Harrison Avenue, SC201, Boston, MA, USA
[b] Neuroscience Program, Sackler School of Graduate Biomedical Sciences, Tufts University, 136 Harrison Avenue, SC201, Boston, MA, USA
[c] Broad Institute, 301 Binney Street, 5066, Cambridge, MA 02142, USA

ARTICLE INFO

Article history:
Received 12 February 2014
Revised 17 July 2014
Accepted 15 August 2014
Available online 23 August 2014

Keywords:
Epilepsy
Glutamate
Freeze lesion
Gabapentin
Thrombospondin
Cortex
Developmental cortical malformation

ABSTRACT

Developmental cortical malformations are associated with a high incidence of drug-resistant epilepsy. The underlying epileptogenic mechanisms, however, are poorly understood. In rodents, cortical malformations can be modeled using neonatal freeze-lesion (FL), which has been shown to cause in vitro cortical hyperexcitability. Here, we investigated the therapeutic potential of gabapentin, a clinically used anticonvulsant and analgesic, in preventing FL-induced in vitro and in vivo hyperexcitability. Gabapentin has been shown to disrupt the interaction of thrombospondin (TSP) with α2δ-1, an auxiliary calcium channel subunit. TSP/α2δ-1 signaling has been shown to drive the formation of excitatory synapses during cortical development and following injury. Gabapentin has been reported to have neuroprotective and anti-epileptogenic effects in other models associated with increased TSP expression and reactive astrocytosis. We found that both TSP and α2δ-1 were transiently upregulated following neonatal FL. We therefore designed a one-week GBP treatment paradigm to block TSP/α2δ-1 signaling during the period of their upregulation. GBP treatment prevented epileptiform activity following FL, as assessed by both glutamate biosensor imaging and field potential recording. GBP also attenuated FL-induced increases in mEPSC frequency at both P7 and 28. Additionally, GBP treated animals had decreased in vivo kainic acid (KA)-induced seizure activity. Taken together these results suggest gabapentin treatment immediately after FL can prevent the formation of a hyperexcitable network and may have therapeutic potential to minimize epileptogenic processes associated with developmental cortical malformations.

Introduction

Developmental cortical malformations, such as polymicrogyria and cortical dysplasia, are a group of neurological disorders with a high incidence of intractable epilepsy (Takano et al., 2006). They are characterized by areas of anatomically disorganized cortex that often evolve into a seizure focus (Leventer et al., 2010). The mechanisms by which these lesions contribute to the onset of seizure activity, however, are poorly understood. To investigate the pathophysiology of cortical malformation, we have utilized the neonatal freeze-lesion (FL) model, which reproduces key features of polymicrogyria including structural abnormalities and cortical hyperexcitability (Jacobs et al., 1996; Luhmann et al., 1998a,b). Briefly, on the day of birth (P0), mice are anesthetized and a freezing probe is applied to the surface of the skull. This results in the formation of a microgyrus at the site of lesion. Epileptiform activity can be evoked in the region adjacent to the lesion (paramicrogyral zone; PMZ) in acute brain slices after a 10- to 11-day latent period (Jacobs et al., 1999). Spontaneous seizures have not been reported in the FL model (but see Kamada et al., 2013) but numerous changes in network connectivity and excitability have been reported (Jacobs and Prince, 2005; Scantlebury et al., 2004).

A number of lines of evidence specifically implicate increased glutamatergic signaling in the pathophysiology of FL-induced hyperexcitability. Increased excitatory input onto both interneurons and pyramidal cells in the PMZ were first reported in the FL model after P14, when acute cortical brain slices generate epileptiform responses (Jacobs and Prince, 2005). Importantly, later studies went on to show that increased excitatory input onto layer V pyramidal cells is present before the onset of epileptiform activity. This supports the hypothesis that network level changes occur during the latent period, before the onset of hyperexcitability at P14 (Zsombok and Jacobs, 2007). Changes in glutamate receptor expression and localization have also been reported in the FL model (Hagemann et al., 2003; Defazio and Hablitz, 2000; Zilles et al., 1998). Excitatory connectivity between cortical layers II and V is specifically increased as assayed by laser-scanning photostimulation (Brill and

* Corresponding author at: Department of Neuroscience, Tufts University School of Medicine, 136 Harrison Avenue, SC203, Boston, MA 02111, USA. Fax: +1 617 636 2413.
Available online on ScienceDirect (www.sciencedirect.com).
[1] Current address.

http://dx.doi.org/10.1016/j.nbd.2014.08.022
0969-9961/

Huguenard, 2010). This implicates local intra-cortical circuitry in the hyperexcitable phenotype. Furthermore, glutamate biosensor imaging studies showed that stimulus-evoked extracellular glutamate levels were increased in the FL cortex (Dulla et al., 2012). Taken together, these reports clearly implicate increased excitatory signaling in the FL model. The specific molecular and cellular changes which occur during the latent period and which drive increased excitatory signaling remain largely unknown. Identifying these mechanisms is important as it will provide novel targets for therapeutic interventions.

To this end, we have begun to investigate the role of neuron/astrocyte signaling following FL. It has been shown that neurons in co-culture with astrocytes form more synapses than when cultured alone (Ullian et al., 2001). This effect can be replicated by the addition of astrocyte-conditioned media (Ullian et al., 2004a,b), implicating an astrocyte-secreted protein in driving synaptogenesis. Thrombospondins (TSPs) were identified as the astrocyte-secreted factors responsible for excitatory synapse formation (Christopherson et al., 2005). TSPs have been shown to promote synaptogenesis in the developing CNS, but their expression decreases dramatically in the adult brain (Christopherson et al., 2005). Following injury in the mature cortex, however, reactive astrocytes re-express TSP (Lin et al., 2003; Zhou et al., 2010). Whether neonatal injury induces similar increases in TSP is unknown. The receptor for TSP-mediated synaptogenesis is the calcium channel subunit α2δ-1 (Eroglu et al., 2009; Christopherson et al., 2005). α2δ proteins are accessory subunits of voltage gated calcium channels, which enhance trafficking to the plasma membrane and can influence biophysical properties of the channels. Interestingly, α2δ-1's role in synaptogenesis appears to be independent from calcium channel association (Hoppa et al., 2012).

Recently, the anticonvulsant and antiallodynic drug gabapentin (GBP) was shown to block the interaction between TSP and α2δ-1 (Eroglu et al., 2009). GBP was originally designed as a GABA-mimetic that could freely cross the blood–brain barrier; however, it was subsequently found to have no actions on GABAergic neurotransmission (Sills, 2006). Rather, its therapeutic actions appear to be mediated by antagonizing the interaction of TSP and α2δ-1 (Eroglu et al., 2009; Eroglu, 2009). Recent studies have shown that GBP treatment prevented injury-induced increases in reactive astrocytosis and excitatory synaptogenesis (Li et al., 2012; Lo et al., 2011). Furthermore, GBP treatment attenuated cortical hyperexcitability in a model of posttraumatic epilepsy associated with upregulation of α2δ-1 (Li et al., 2012). Given these findings, along with reports of increased reactive astrocytes in the FL model (Bordey et al., 2001; Campbell and Hablitz, 2008; Dulla et al., 2012), we hypothesized that treating FL animals with GBP during the latent period may attenuate later hyperexcitability in the FL model. We found that both TSP and α2δ-1 immunoreactivity were increased focally 3 and 7 days following FL. We therefore treated FL animals with GBP for one week (P1–P7) and then assessed epileptiform activity and glutamate signaling in acute brain slices (P14–P28) and seizure susceptibility in vivo (>P60). We found that GBP treatment after FL caused long-term decreases in both in vitro and in vivo hyperexcitability. GBP treatment also prevented FL-induced increases in mEPSC frequency. Taken together these results suggest that GBP treatment protects against the onset of hyperexcitability associated with developmental cortical malformation, potentially through the inhibition of TSP/α2δ-1 signaling.

Materials and methods

Production of glutamate FRET biosensor

BL21(DE3) bacteria were transformed with pRSET-FLII^{81}E-1 μ plasmids and streaked on an LB plate with ampicillin (100 μg/ml) (Dulla et al., 2008). After overnight incubation at 37 °C, a single colony was picked and grown in 1 l LB with ampicillin (100 μg/ml) for 3 days at 25 °C in the dark with rapid shaking (300 rpm). Cells were harvested by centrifugation, resuspended in extraction buffer (50 mM Sodium Phosphate, 300 mM NaCl, pH 7.2), and lysed with CelLytic B reagent (Sigma). The FRET sensor was purified by Talon His-affinity chromatography (Clontech). Binding to the resin was performed in batch at 4 °C, washed in a column with extraction buffer, and then eluted with extraction buffer containing 150 mM imidazole.

Animals and freeze lesion surgery

Experimental microgyri in primary somatosensory cortex (right hemisphere) were induced in P0 C57BL/6 mouse pups by freeze lesioning as described previously in rats (Dulla et al., 2012) and other mice FL models (Wang et al., 2012), but with some modifications. Briefly, animals were anesthetized by hypothermia, an incision into the scalp was made, and a copper probe (1 mm X 1.5 mm) cooled to −50 to −60 °C was placed onto the exposed skull for 5 s. Sham operated littermates were generated by leaving the probe at room temperature. After freeze-lesioning, the incision was closed using surgical glue, and pups were warmed and returned to the dam. Mice were treated with once daily i.p. injections of either gabapentin (200 mg/kg) or vehicle from P1 to P7. All guidelines of Tufts University's Institutional Animal Care and Use Committee were followed.

Preparation of brain slices

Cortical brain slices containing sensorimotor cortex (400 μM) were prepared from C57BL/6 mice (P3–P30) of either sex. Briefly, mice were anesthetized with isoflurane, decapitated, and the brains were rapidly removed and placed in chilled (4 °C) low-Ca, low-Na slicing solution consisting of (in mM): 234 sucrose, 11 glucose, 24 $NaHC0_2$, 2.5 KCl, 1.25 NaH_2PO_4, 10 $MgSO_4$ and 0.5 $CaCl_2$, equilibrated with a mixture of 95% O_2:5% CO_2. The brain was glued to the slicing stage of a Vibratome 3000 sectioning system and slices were cut in a coronal orientation. The slices were then incubated in 32 °C oxygenated aCSF (in mM: NaCl, 126, KCl, 2.5, NaH_2PO_4, 1.25, $MgSO_4$, 1, $CaCl_2$, 2, glucose, 10, $NaHCO_2$, 26) for 1 h, and then allowed to cool to room temperature and subsequently used for sensor loading and recording.

Loading of FRET-based glutamate sensor protein

Loading of glutamate biosensor was done as previously described (Dulla et al., 2008). A 35 mm tissue culture dish was filled with ≈2 ml aCSF and a 0.4 μm Millicell (Millipore) culture plate was inserted. Care was taken to ensure that no bubbles were present under the plate insert and that no aCSF spilled onto its top surface. A single brain slice was transferred from the incubation chamber onto the plate insert and excess aCSF was removed. The dish containing the slice was then placed in a humidified and warmed (32 °C) chamber equilibrated with 95% O_2:5% CO_2. 50 μl of concentrated glutamate FRET sensor protein (≈50 ng/μl) was then carefully applied to the top surface of the slice. After 5–10 min of incubation, slices were removed from the loading chamber and placed into the recording chamber.

Field recordings

Slices were placed in an interface chamber maintained at 34 °C, superfused with oxygenated aCSF at 2 ml/min and cortical projections were stimulated with a tungsten concentric bipolar electrode at the layer VI–white matter boundary. Electrical stimulation consisted of 10–50 μA, 100 μs pulses at 30 s intervals delivered by a stimulus isolator (World Precision Instruments). Glass micropipettes (resistance ≅ 1 MΩ) were filled with aCSF and placed in layer V of the cortex directly above the stimulation electrode. Electrophysiological data were recorded with an Axon Multiclamp 700A amplifier and Digidata 1322A digitizer (sampling rate = 20 kHz) with pClamp software (Molecular Devices). Threshold

stimulation intensity was identified as the minimum amount of current required to elicit a detectable cortical field potential response (≥0.05 mV).

Biosensor imaging

Collection of glutamate biosensor data was done as previously described (Dulla et al., 2008). Slices were placed into the recording chamber of an Olympus BX51WI microscope with continual superfusion of aCSF for simultaneous imaging with an Olympus 4× objective. Excitation with 440 nm wavelength light was used. A NeuroCCD camera (RedShirt Imaging) was used to collect 40 × 80 pixel imaging data at 1000 Hz. Each imaging experiment consisted of collecting five movies each containing 1500 frames with 30 s between movies. Each captured 1500 ms movie contained a 90 ms period of dark noise (camera signal before shutter opening) captured before fluorescence was turned on. Fluorescence was turned on for 1210 ms, and then turned off for 200 ms. Slices were stimulated 250 ms after fluorescence was turned on. Emission signals first passed through a 455 nm DCLP dichroic mirror to eliminate excitation fluorescence and were then separated into two channels using a Photometrics Dual-View or Optosplit two channel imaging system to isolate cyan fluorescent protein (CFP) and Venus, a variant of yellow fluorescent protein (YFP) signals. Ratiometric images of CFP/Venus signals were created and analyzed as described below.

Patch clamp recordings

Slices were placed in the recording chamber of an Olympus BX51 microscope with continual superfusion of oxygenated aCSF maintained at 32 °C. Layer V pyramidal neurons were visually identified with infrared differential interference contrast (DIC) microscopy and whole cell patch-clamp recordings were made with a borosilicate glass electrode (3–5 MΩ) filled with (in mM): 140 CsMs, 10 HEPES, 5 NaCl, 0.2 EGTA, 5 QX314, 1.8 MgATP, 0.3 NaGTP and pH 7.25. The recording electrode was placed approximately 200 μm from the site of injury in the PMZ. Data was collected using an axon Multiclamp 700B amplifier, Digidata 1440A digitizer and pClamp software. Miniature EPSCs were recorded in the presence of 1 μM TTX at a holding potential of −70 mV. Only recordings with an access resistance that varied <20% were accepted for analysis.

Electrophysiological data analysis

Field recordings were analyzed using pClamp (Axon Instruments) and MATLAB software. Traces were recorded at threshold stimulation, the minimum stimulation required to elicit a detectable response, and at 2× and 10× threshold stimulation. Stimulus duration was 100 μs for all studies. Amplitude was defined as the maximum negative voltage change following electrical stimulation, while duration was defined as the amount of time following stimulation for the response to return to baseline. Area under the curve was used to determine the integrated network activity and was calculated by integrating the extracellular field potential during the first 1000 ms following initial stimulation. mEPSC recordings were analyzed using Clampfit (Axon Instruments Inc.) and Mini Analysis (Synaptosoft). Recordings of 60–120 s were analyzed for average amplitude and inter-event frequency.

Glutamate imaging data analysis

Imaging data was analyzed using customized MATLAB software. Raw imaging data was first split into CFP and Venus and the ratio of the two fluorophores was computed. An average pre-stimulation ratio image was then made by averaging the 40 ms of imaging data prior to the stimulus. The pre-stimulation image was then subtracted from all images resulting in a ΔFRET image. Processed ΔFRET images were then converted into $\Delta FRET_{signal}/\Delta FRET_{noise}$ data, pixel-by-pixel, by dividing all time-points by the standard deviation of ΔFRET during the pre-stimulus time period. Imaging data was then analyzed to determine the peak amplitude of the signal.

Immunohistochemistry

Fixed mouse brains were prepared by either submersion fixation (P3) or transcardial perfusion (P7–P60) with 4% paraformaldehyde. Fixed brains were sectioned at 40 μm using a Thermo Fisher Microm HM 525 cryostat. Brain sections were blocked using blocking buffer (5% normal goat serum, 1% bovine serum albumin, in PBS) for 1 h at room temperature. Thrombospondin1/2 (1:250, Abcam), α2δ-1 (1:500, Abcam), GFAP (1:500, Abcam), and NeuN (1:1000, Millipore) antibodies were diluted in PBS with 2% Triton-X 100 and 5% blocking buffer. Cortical sections were incubated with diluted primary antibodies overnight at 4 °C. Secondary antibodies (goat anti-rabbit Cy3.5, goat-anti mouse FITC, Jackson Labs) were diluted in PBS with 5% blocking buffer and added to cortical sections for 2 h at room temperature. Slices were mounted using Vectashield (Vector Labs) and imaged with a Nikon A1R confocal microscope using consistent laser intensity and imaging setting across samples. Data was analyzed using Nikon software and regions of interest of approximately 500 μm^2 were drawn in the cortex spanning from the white matter to layer I. Average intensity of staining within the region of interest was compared to the relative intensity of staining in sham injured animals at each time point.

Kainic acid-induced epileptiform activity and EGG recordings

Six week old freeze lesion and sham control littermates were implanted for electroencephalogram (EEG) recording based on a Tufts Institutional Animal Care and Use Committee approved protocol. Briefly, animals were anesthetized (100 mg/kg ketamine and 10 mg/kg xylazine). An incision was made on the scalp and a headmount (Pinnacle Technology) was fixed to the skull using four screws and dental cement. The locations of the EEG screws were as follows: two screws were placed in each hemisphere anterior to bregma, and two screws were placed in each hemisphere posterior to bregma. Signals from these screws were used to generate differential EEG recordings. Following surgery, the animals were given 5–7 days to recover. EEG recordings were acquired using a 100× gain preamplifier high-pass filtered at 1.0 Hz (Pinnacle Technology). A baseline EEG was recorded for 1 h and then animals were given an intraperitoneal injection of 20 mg/kg kainic acid (KA; Sigma). Animals were perfused one day following KA injection and the brains were collected for immunohistochemical analysis. Epileptiform activity was measured posthoc as previously described (Lee and Maguire, 2013; Klaassen et al., 2006; Maguire et al., 2005; Maguire and Mody, 2009).

KA-induced seizures were defined by rapid onset of high-amplitude activity (2.5× the standard deviation of the baseline) and were only counted if they lasted longer than 5 s. Quantification of seizure activity was also based on the changes in power of the fast-Fourier transform of the EEG. EEG activity that was abnormal, but that did not meet the criteria to be included as a seizure, was also included in the analysis of epileptiform activity. This included periods of rhythmic spiking lasting longer than 30 s. This set of criteria is similar to published reports from other groups (Castro et al., 2012). Seizure latency was defined as the time from KA injection to the onset of the first electrographic seizure. Total time exhibiting epileptiform activity (% epileptiform activity) was computed as the integrated time of all epileptiform and ictal activity during the 2 hour recording period divided by 120 min. Seizure duration was defined as the time from the initiation of an individual episode for the epileptiform EEG pattern until the return to baseline. These values were averaged across all recorded seizures on an animal by animal basis. LabChart Pro software (ADInstruments) was used for data acquisition and analysis. Spectral analysis was performed using

Fast Fourier Transforms in MATLAB. 6 second non-overlapping windows were used to generate average power spectra for both the pre-KA treatment and the 2 hour EEG recording following KA injection. Mean power spectra were then normalized to the average power from 18 to 80 Hz and binned in 0.25 Hz bins. Mean spectra for each animal was then averaged together for each treatment condition for control and KA EEG. KA mean EEG was then normalized frequency bin by frequency bin to pre-KA EEG and t-tests were performed on individual frequency bins.

Statistical analysis

For comparison between two experimental groups, a Student's t-test was used. For three or more experimental groups, a one-way ANOVA with the Tukey post-hoc test was used. For comparison of cumulative probabilities, a Kolmogorov–Smirnov test was used. Values of $p < 0.05$ or more were considered statistically significant.

Drugs and reagents

All salts and glucose for buffers were obtained from Sigma-Aldrich. Gabapentin was obtained from Abcam Biochemicals.

Results

Thrombospondin and α2δ-1 immunoreactivity are increased after FL

Astrocyte-secreted thrombospondins regulate excitatory synapse formation in the developing CNS (Christopherson et al., 2005; Eroglu et al., 2009) and they have been shown to be upregulated following injury correlated with an increase in reactive astrocytosis (Lin et al., 2003; Li et al., 2012). To establish if thrombospondin levels are altered in our model, freeze lesion and sham lesion brains were probed for thrombospondin 1 and 2 (TSP1/2) immunoreactivity. We found significant increases in TSP1/2 immunofluorescence in FL cortex 3 (Figs. 1A, B; 2.21 ± 0.056 fold increase compared to sham, n = 3; p < .001) and 7 days following FL (1.81 ± 0.173 fold increase compared to sham, n = 9; p < .05). Diffuse TSP1/2 staining was observed in the injured area, nearby GFAP immunoreactivity (Fig. 1C). The immunoreactivity of TSP's neuronal receptor, the α2δ-1 subunit of voltage gated calcium channels, was also significantly increased 3 (Figs. 1D, E; 1.88 ± 0.135 fold increase compared to sham, n = 6; p < .001) and 7 days following FL (1.57 ± 0.246 fold increase compared to sham, n = 4; p < .05). By P14, there were no longer any significant differences in TSP1/2 or α2δ-1 immunoreactivity. These results indicate that both TSP1/2 and α2δ-1 immunoreactivity are increased in the neocortex following FL at the site of injury during the latent period. Therefore, they may play a role in pathological network reorganization. To address this question, we next designed a treatment paradigm to block the interaction of TSP with α2δ-1.

Gabapentin treatment decreases network hyperexcitability following FL

Freeze lesion and sham injured animals were given daily intraperitoneal (i.p.) injections of either gabapentin (GBP, 200 mg/kg), which blocks the interaction between TSP and α2δ-1 (Gee et al., 1996) or vehicle from P1 to P7. This treatment regimen was designed to coincide with the period of increased TSP1/2 and α2δ-1 immunoreactivity. No changes in developmental weight gain or obvious behavioral changes associated with GBP treatment were seen. To investigate the effect of this treatment on network hyperexcitability, we first examined evoked field excitatory post-synaptic potentials

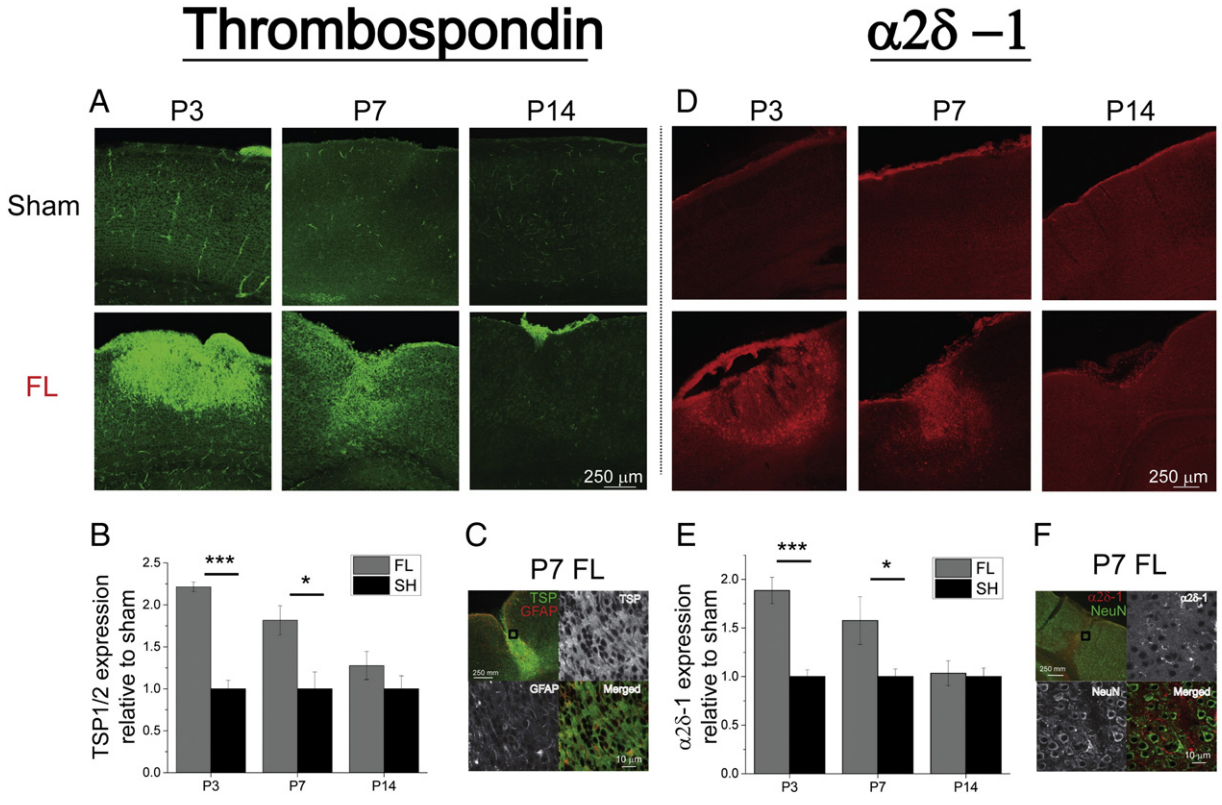

Fig. 1. Thrombospondin and α2δ-1 immunoreactivity are increased after FL. (A) TSP1/2 staining in sham injured and FL cortex at P3, P7 and P14. (B) Average TSP1/2 fluorescence relative to sham. (C) TSP1/2 (green) and GFAP (red) co-stain of a P7 FL animal and 60× magnification of the area in the black box for TSP1/2, GFAP and merged TSP1/2 (green) and GFAP (red). (D) α2δ-1 staining in sham injured and FL cortex at P3, P7 and P14. (E) Average α2δ-1 fluorescence relative to sham. (F) α2δ-1 (red) and NeuN (green) co-stain of a P7 FL animal and 60× magnification of the area in the black box for α2δ-1, NeuN and merged α2δ-1 (red) and NeuN (green), ***p < 0.001, *p < 0.05.

(fEPSPs) in acute brain slices from FL animals between P14 and P28. This was between 1 and 3 weeks after treatment with GBP was discontinued. Stimulation intensity was set based on the minimum stimulation required to evoke a detectable fEPSP (threshold (TH) stimulation, see Materials and methods). TH stimulation intensity was not significantly different across experimental conditions. Epileptiform activity was defined as fEPSPs which contained high frequency activity, as well as increased peak amplitude and duration (Fig. 2A). The frequency of epileptiform activity was calculated as the percentage of fEPSPs that were epileptiform per slice. Brain slices from freeze lesion animals exhibited a significantly higher percentage of epileptiform fEPSPs (Fig. 2B; 54.83 ± 8.44%, n = 25) compared to slices from sham injured animals (12.02 ± 6.12%, n = 18; $p < .001$). Strikingly, slices from GBP-treated FL animals had a significantly decreased amount of epileptiform activity compared to slices from vehicle-treated FL animals (13.62 ± 5.24%, n = 19; $p < .01$). There was no significant difference in the percentage of epileptiform activity in slices from GBP treated FL animals and sham injured animals. As a more quantitative measure of epileptiform activity, the areas of the fEPSPs were also calculated. fEPSPs from vehicle treated FL animals were significantly larger in area (Fig. 2C, 22.91 ± 4.38 mV ms) compared to sham (9.56 ± 1.21 mV ms) and GBP treated FL animals (9.94 ± 1.45 mV ms; $p < .05$). No significant differences in fEPSP areas were observed between sham and GBP treated FL animals. Taken together, these results indicate that GBP treatment is able to reduce in vitro cortical hyperexcitability following FL.

Gabapentin treatment preserves cortical input–output relationships after FL

We next examined the input–output relationship after FL by recording evoked fEPSPs at threshold, 2×, and 10× threshold stimulus intensities. An increase in stimulation will normally elicit a correspondingly larger fEPSP. In sham-lesioned animals, acute cortical slices had normal input output relationships. 2× threshold stimulation evoked a significantly larger fEPSP (17.98 ± 2.17 mV ms, $p < 0.05$) as compared to threshold stimulation (Fig. 2D). In FL animals, however fEPSP area at 2× stimulation (29.45 ± 4.79 mV ms) was not significantly different from threshold stimulation. These results suggest that the ability of the FL cortex to generate controlled, scaled responses to input is lost and that epileptiform activity is evoked in an all-or-none manner. The typical input–output relationship was restored in GBP treated FL animals, suggesting that GBP treatment after FL protects against pathological changes in cortical network function. When stimulation was increased to 10× threshold, fEPSPs from sham and FL cortex were indistinguishable, as has been previously reported in this model (Jacobs et al., 1999), likely due to increased engagement of inhibitory circuitry. At 10× threshold stimulation, GPB treatment did not alter fEPSPs (data not shown).

Gabapentin treatment decreases evoked extracellular glutamate signaling as measured using FRET based biosensor imaging

Previous studies utilizing high-speed glutamate biosensor imaging have shown an increase in stimulus evoked changes in extracellular glutamate levels in FL cortex compared to sham lesioned cortex (Dulla et al., 2012). The glutamate biosensor is a FRET-based fluorophore which allows us to monitor changes in extracellular glutamate signaling. Using this approach, we loaded acute cortical brain slices from GBP and vehicle treated FL mice with glutamate biosensor protein and performed glutamate imaging with simultaneously evoked extracellular field potential recordings. Glutamate signaling was analyzed by generating images of the ΔFRET (CFP/Venus ratio) signal divided by the ΔFRET noise on a pixel-by-pixel basis (Fig. 3A). Traces were then

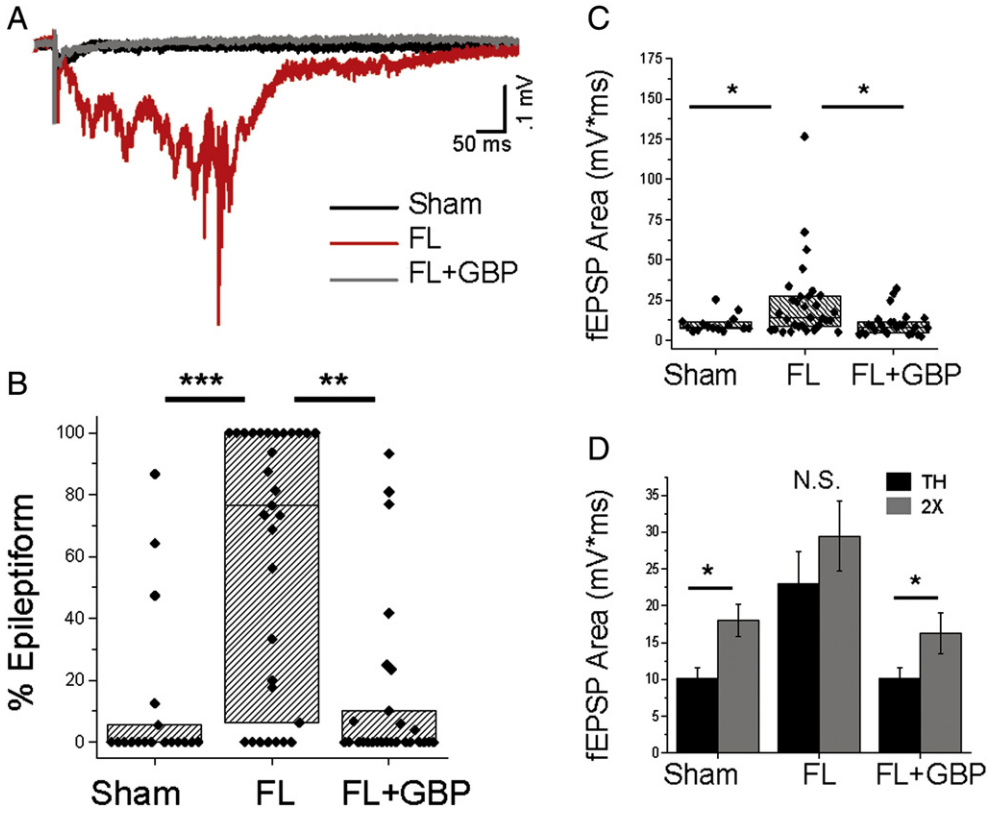

Fig. 2. Gabapentin treatment decreases network hyperexcitability following FL. (A) Representative evoked field excitatory post-synaptic potentials (fEPSPs) recorded in the neocortex from sham injured (black), FL (red) and GBP treated FL animals (gray). (B) Box–Whisker plot of percent of stimulus-evoked fEPSPs which had epileptiform activity in acute brain slices at threshold stimulation, $^{**}p < 0.01$, $^{***}p < 0.001$. (C) Box–Whisker plot of fEPSP area (integrated area under the curve 1 s post-stimulation) at threshold stimulation, $^{*}p < 0.05$. (D) Average fEPSP area at threshold and 2× threshold stimulation for sham, FL and GBP treated FL animals, $^{*}p < 0.05$.

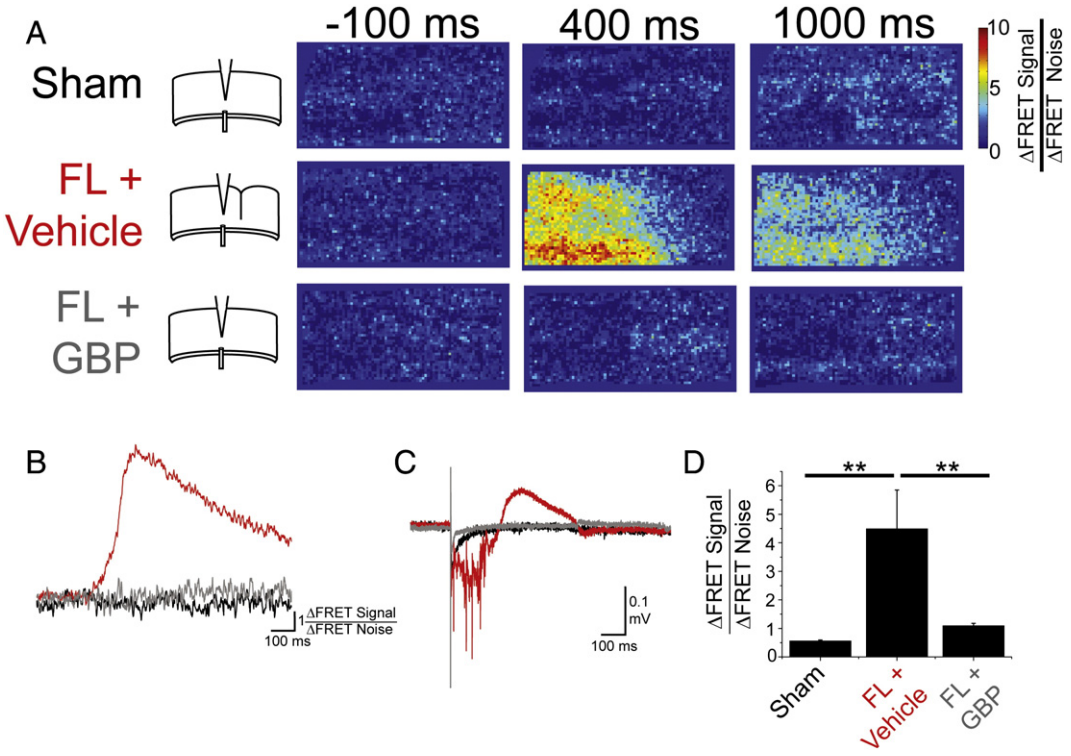

Fig. 3. Gabapentin treatment decreases evoked extracellular glutamate signaling as measured using FRET based biosensor imaging. (A) Glutamate images of ΔFRET (CFP/Venus ratio) signal/ΔFRET noise on a pixel-by-pixel basis at 100 ms pre-stimulation, 400 ms post-stimulation and 1000 ms post-stimulation in sham, vehicle and GBP treated animals. Diagram illustrates cortical area being imaged with placement of recording electrode in cortical layer IV/V and stimulating electrode in the underlying white matter. (B) Individual ΔFRET signal/noise traces from sham (black), FL + Veh (red) and FL + GBP (gray) slices. (C) and simultaneously recorded evoked fEPSPs. (D) Average peak amplitude of ΔFRET signal/noise, $^{**}p < 0.01$.

generated by plotting the $\Delta FRET_{signal}/\Delta FRET_{noise}$ over time and differences in the peak glutamate signal were quantified by calculating the maximum amplitude of each glutamate transient (Figs. 3B, D). The peak glutamate signal from slices of vehicle treated FL animals (4.46 ± 1.35 $\Delta FRET_{signal}/\Delta FRET_{noise}$, $n = 6$) was significantly increased when compared to sham injured (0.56 ± 0.33, $n = 4$; $p < .001$) and GBP treated FL animals (1.09 ± 0.08, $n = 12$; $p < .01$). These differences in glutamate signal complement the paired electrophysiological field data (Fig. 3C). Large changes in extracellular glutamate signal are associated with high amplitude and polyphasic field potentials, while small changes in the glutamate signal coincide with field potentials that are small in amplitude and duration. The reduced levels of stimulus evoked extracellular glutamate in GBP versus vehicle treated animals suggest that GBP treatment has decreased the glutamatergic neurotransmission associated with epileptiform field activity following FL.

An anticonvulsant with a different mechanism of action does not replicate the effects of gabapentin

Since gabapentin has anticonvulsant properties, we wanted to address the specificity of the observed decrease in hyperexcitability following FL by treating animals with an anticonvulsant that does not affect the TSP and α2δ-1 signaling pathway. Phenobarbital is a widely used antiepileptic drug, which acts by potentiating inhibition mediated by $GABA_A$ receptors and thus inhibiting excitation mediated by AMPA receptors (Macdonald and Barker, 1978). Phenobarbital has not been shown to affect α2δ-1 signaling. Freeze lesion and sham injured animals were given daily i.p. injections of phenobarbital (20 mg/kg) or saline, from P1 to P7 to establish if anticonvulsant treatment following FL is sufficient to prevent the formation of a hyperexcitable network. No changes in developmental weight gain or obvious behavioral changes associated with phenobarbital treatment were seen. Hyperexcitability was assessed by recording evoked cortical field potentials at P28 (Fig. 4). We found that there was no significant decrease in the percentage of epileptiform activity in the phenobarbital treated FL animals (Fig. 4B; $53.52 \pm 11.31\%$, $n = 17$) as compared to the vehicle treated FL animals ($64.28 \pm 12.61\%$, $n = 14$). fEPSPs from phenobarbital treated FL animals were also significantly larger in area (Fig. 4C; 17.48 ± 3.32 mV ms) compared to sham injured animals (6.61 ± 0.45 mV ms; $p < .01$) and had no significant differences compared to vehicle treated FL animals (20.03 ± 4.35 mV ms). These results suggest that the effects of gabapentin on decreasing network hyperexcitability are not due to a general anticonvulsant mechanism.

Gabapentin treatment decreases the frequency of excitatory postsynaptic currents in layer V pyramidal neurons of the FL cortex

We next examined miniature excitatory postsynaptic currents (mEPSCs) in layer V pyramidal neurons of the PMZ or isotopic regions in sham-lesioned animals. Slices were perfused with normal aCSF containing 1 μm TTX in the bathing medium and recorded cells were held at −70 mV. At P7, there were no differences in mEPSC amplitude between sham, FL and GBP treated FL animals (Figs. 5B, C; 16.39 ± 0.39 pA, $n = 7$; 18.03 ± 0.86, $n = 10$ and 16.45 ± 1.27, $n = 14$ respectively). At P7, FL caused a significant leftward shift in the cumulative probability distribution of inter-event interval compared to sham animals, indicating a significant increase in mEPSC frequency (Fig. 5D, $p < .001$). Treatment with GBP in FL animals caused a significant rightward shift in the cumulative probability distribution, showing that GBP treatment decreased mEPSC frequency (Fig. 5D, $p < .001$). At P28, the average mEPSC amplitude was significantly increased in FL slices compared to sham slices (Figs. 5F, G; 16.64 ± 1.14 pA, $n = 8$ vs. 13.49 ± 0.58, $n = 7$; $^{*}p < .05$). Interestingly, this increase in amplitude was not altered by GBP treatment (16.39 ± 1.07 pA, $n = 9$). Consistent

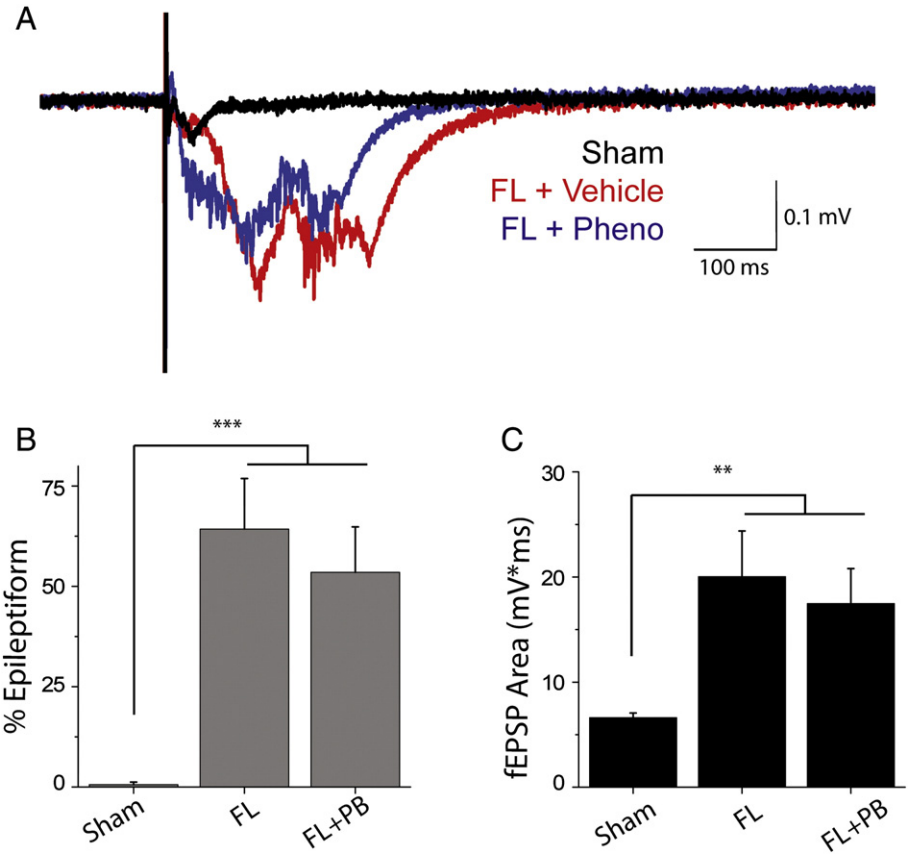

Fig. 4. An anticonvulsant with a different mechanism of action does not replicate the effects of gabapentin. (A) Example evoked cortical field potential from sham (black), FL (red) and phenobarbital treated FL (blue). (B) Epileptiform activity (%) in acute brain slices, ***$p < 0.001$. (C) fEPSP area, **$p < 0.01$.

with previous results (Jacobs and Prince, 2005), we found that mEPSC frequency was increased at P28 following FL as compared to sham (Fig. 5H, $p < .001$). Again, GBP treatment significantly decreased mEPSC frequency at P28 (Fig. 5H, $p < .001$). The longer inter-event intervals at both time points show that one week of GBP treatment is sufficient to decrease the frequency of mEPSCs at P7 and to have a long-lasting protective effect against FL-driven increases in mEPSC frequency. These results are consistent with the hypothesis that excitatory drive onto pyramidal neurons of cortical layer V in the PMZ is increased following FL and that GBP treatment attenuates this increase.

Gabapentin treatment decreases GFAP immunoreactivity following FL

Previous work has shown that astrocyte density is altered after FL and that there is an increase in reactive astrocytes in the FL cortex as assessed by GFAP immunoreactivity (Dulla et al., 2012; Bordey et al., 2001). Consistent with previous results, we found a significant increase in GFAP-positive pixels in slices from FL animals compared to sham injured animals at P7 (Fig. 6; 61.70 ± 9.94%, n = 5 vs. 1.04 ± 0.47, n = 3; $p < .01$). GFAP immunoreactivity remained elevated at P14 (36.35 ± 6.32, n = 6 vs. 3.95 ± 1.35, n = 2; $p < .01$) and at P28 (32.34 ± 5.67, n = 5 vs. 5.19 ± 4.11, n = 3; $p < .01$). GBP-treated FL animals had a significantly higher number of GFAP-positive pixels (46.85 ± 11.54, n = 4; $p < .05$) as compared to sham injured animals at P7 and did not differ from the vehicle treated FL animals at this time point. This increase in reactive astrocytes shortly after FL is not surprising as GBP may antagonize the TSP signaling pathway downstream of astrocyte activation. At later time points, there were significantly less GFAP-positive pixels in the GBP treated FL animals as compared to vehicle treated FL animals (10.93 ± 3.62, n = 5; $p < .01$ at P14 and 16.09 ± 3.26, n = 7; $p < .01$ at P28). These results suggest that while treatment with GBP does not protect against the initial rise in GFAP expression associated with acute injury-induced reactive astrocytosis, it is able to attenuate the long term increase in GFAP expression and suggests a suppression of later reactive astrocytosis.

Gabapentin treatment decreases in vivo kainic acid-induced seizure activity

One limitation of the neonatal FL model is that despite showing reliable in vitro hyperexcitability, these animals do not demonstrate spontaneous behavioral or electrographic seizure (Kellinghaus et al., 2007). Therefore, to assess in vivo hyperexcitability, EEG recordings were performed before and after acute i.p. kainic acid (KA) injection (20 mg/kg) to examine chemically-induced seizure activity in adult FL and sham injured animals. Briefly, FL and sham surgeries were performed at P0, GBP treatment occurred from P1–P7. EEG electrodes were implanted at 6 weeks of age and KA injections were given at 7 weeks of age. Power spectra were calculated from the 2 hour time window following KA injection (Figs. 7A–C). FL animals spent significantly more time seizing (Fig. 7D; 71.01 ± 5.64%, n = 7) compared to sham injured animals (35.69 ± 8.29, n = 7; $p < .01$) and on average had seizures that were longer in duration (Fig. 7E; 399.09 ± 72.72 s vs. 146.81 ± 27.96 s, $p < .01$), demonstrating that FL animals have an increased seizure phenotype in response to acute KA injection. This increase in KA induced seizure activity was completely precluded in the GBP treated FL animals. Animals treated with GBP spent significantly less time seizing (17.87 ± 4.51%; $p < .001$) and displayed shorter average seizure durations (81.07 ± 11.42 s, n = 7; $p < .001$) in comparison to the vehicle treated FL animals. Interestingly,

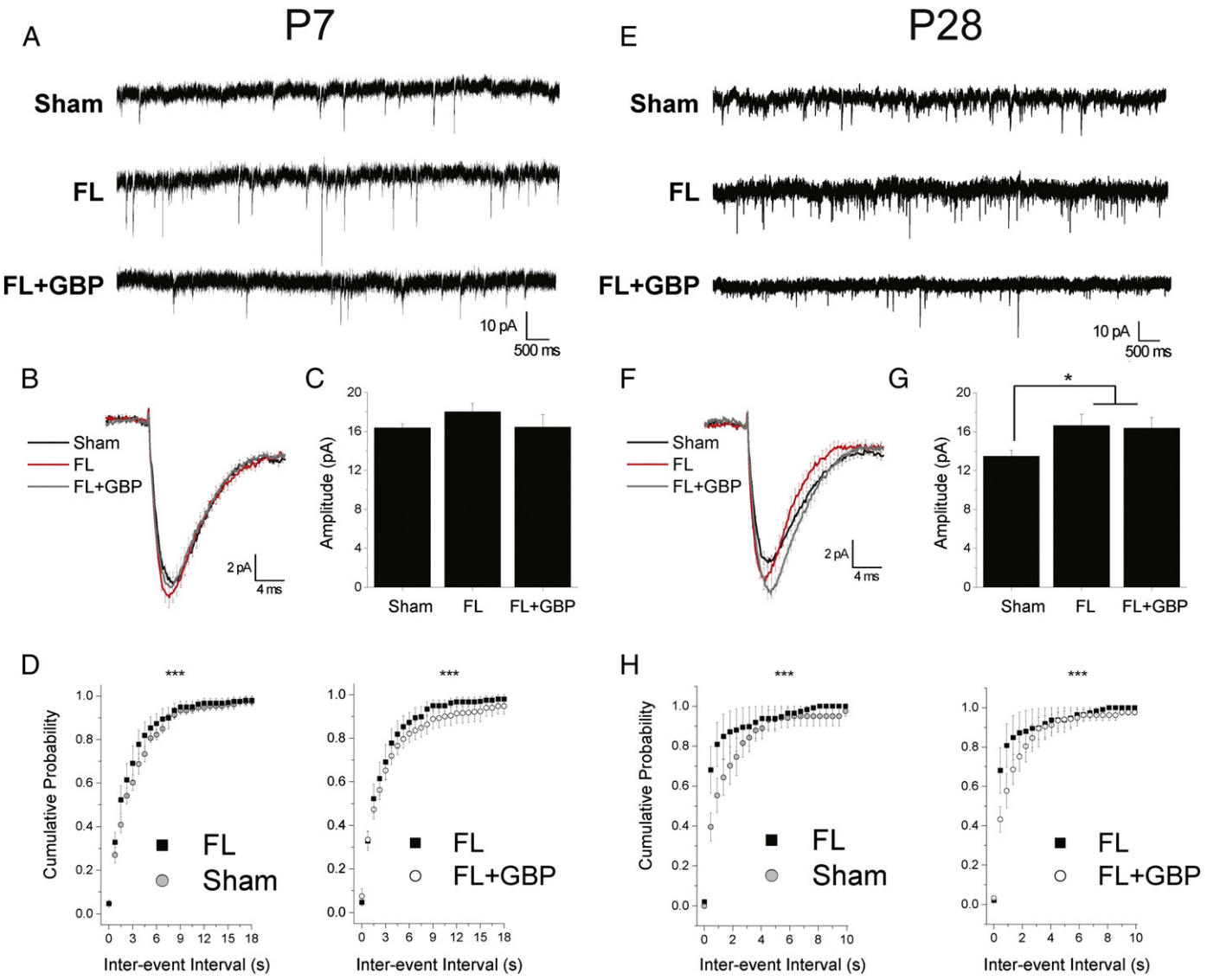

Fig. 5. Gabapentin treatment decreases the frequency of excitatory postsynaptic currents in layer V pyramidal neurons of the FL cortex. (A) Representative mEPSC recording of layer V pyramidal neuron from sham, FL and GBP treated FL cortex at P7. (B) Averaged mEPSC from sham (black), FL (gray) and GBP treated FL (blue) animals at P7. (C) Average mEPSC amplitude at P7. (D) Cumulative probability of inter-event intervals of FL and sham animals ($p < 0.001$ with $D = 0.6656$) and FL and GBP treated FL animals at P7 ($p < 0.001$ with $D = 0.7848$). (E) Representative mEPSC recording of layer V pyramidal neuron from sham, FL and GBP treated FL cortex at P28. (F) Averaged mEPSC from sham (black), FL (gray) and GBP treated FL (blue) animals at P28. (G) Average mEPSC amplitude at P7, $^*p < 0.05$. (H) Cumulative probability of inter-event intervals of FL and sham animals ($p < 0.001$ with $D = 0.3706$) and FL and GBP treated FL animals at P28 ($p < 0.001$ with $D = 0.5994$).

spectral analysis of the EEG signals showed that GBP specifically suppressed theta activity (4–8 Hz) during KA-induced seizures (Fig. 7F). These results suggest that neonatal GBP treatment after FL is able to attenuate adult in vivo hyperexcitability.

Gabapentin treatment protects against cortical tissue loss following acute kainic acid injection

FL animals given an acute KA injection exhibited a remarkable loss of cortical tissue in the area of the lesion 1 day following KA treatment (Fig. 8B). Cortical tissue loss was quantified using cortical sections immunolabeled for NeuN, a neuronal marker. NeuN intensity was not investigated, but rather was used as a way to visualize the cortical mantle. Area of tissue loss was quantified based on the region of cortex absent in the NeuN stain. When the surface of the cortex was completely absent, the area was quantified based on the predicted location of the cortical surface. FL animals demonstrated a significant increase in cortical area lost after KA injection compared to saline-injected FL animals (Fig. 8D, 42.56 ± 9.13 mm^2, $n = 6$ vs. 3.12 ± 0.28, $n = 4$; $p < .01$). Cortical tissue loss following KA treatment was significantly attenuated in GBP treated FL animals (Figs. 8C and D; 2.85 ± 0.64 mm^2, $n = 4$; $p < .001$) compared to the vehicle treated FL animals. These results suggest that GBP treatment from P1 to 7 prevented later susceptibility to KA-induced cortical tissue loss.

Discussion

Here we investigated the effects of in vivo GBP treatment on in vitro and in vivo hyperexcitability caused by neonatal FL. We found that following FL, TSP and α2δ-1 levels were transiently increased; a change temporally correlated with abundant reactive astrocytosis. Because TSP and α2δ-1 are increased during early cortical development in the FL model, they are well-poised to play a role in the formation of a hyperexcitable network. We therefore treated sham and FL animals for one week with GBP, a clinically used anticonvulsant and an antagonist of

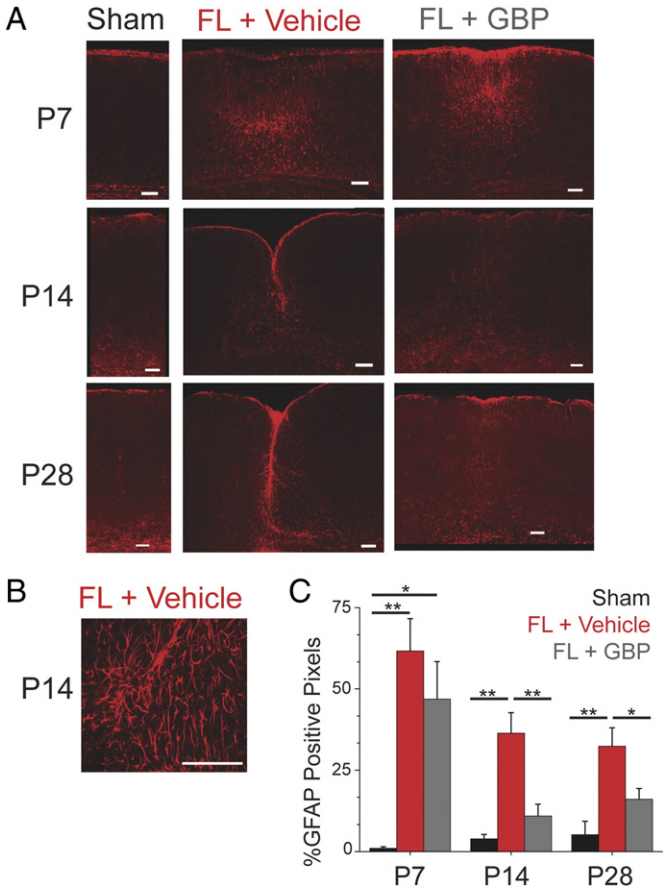

Fig. 6. Gabapentin treatment decreases GFAP immunoreactivity following FL. (A) Representative images of GFAP staining of cortex from sham, vehicle treated FL and GBP treated FL animals at P7, P14 and P28. Scale bar = 100 μm. (B) Higher magnification of GFAP staining from microgyrus of P14 FL cortex. (C) Percent of GFAP positive pixels in 200 μm ROI centered around lesion or equivalent cortical area, $^{*}p < 0.05$, $^{**}p < 0.01$.

TSP/α2δ-1 signaling (Eroglu et al., 2009). This treatment paradigm coincided temporally with the upregulation of TSP and α2δ-1. GBP treatment caused a striking decrease in evoked epileptiform fEPSPs and extracellular glutamate signaling as assayed in acute brain slices. Furthermore, GBP treatment was able to decrease excitatory input onto layer V pyramidal neurons as assessed by changes in the frequency of mEPSCs. Lastly, we found that FL animals had an increased seizure phenotype and significant cortical tissue loss in response to in vivo kainic acid administration. Neonatal treatment with GBP significantly reduced both these pathologies. Taken together, these studies show that GBP-treatment attenuates many of the pathologies associated with neonatal freeze lesion including long-lasting reductions in both in vitro and in vivo measures of hyperexcitability.

Changes in excitation that occur during the two-week latent period, prior to the onset of epileptiform activity, are of particular interest. These changes may both drive later hyperexcitability and be useful targets for therapeutic intervention. We and others have shown that increases in EPSCs occur in the neonatal FL cortex by P7–P11 (Zsombok and Jacobs, 2007). This is in line with the hypothesis that increased excitatory input occurs during the latent period and may drive later hyperexcitability. Increased TSP and α2δ-1 immunoreactivity during the latent period suggest a potential mechanism for induction of hyperexcitability. GBP sensitivity during this time window is consistent with this hypothesis. Is GBP a potentially useful therapeutic target for developmental cortical malformations? There are a number of translational considerations that must first be considered. First, for GBP to have a protective effect, one would predict that both TSP and α2δ-1 would have to be increased. Whether injury upregulates TSPs and α2δ-1 is unknown, but human glial cells are known to express TSPs (Asch et al., 1986) and human endothelial cells upregulate TSP expression in response to oxidative stress (Ning et al., 2011). Second, the results we report here are in a model which has not been reported to have spontaneous seizures. Whether GBP would be efficacious in attenuating seizures associated with developmental cortical malformations remains to be seen. Lastly, patients with cortical malformations often present clinically when seizures begin (Guerrini and Dobyns, 2014). In this situation, GBP treatment would likely not be beneficial as the window for effective intervention may have passed. As neuroimaging and other developmental diagnostics improve, however, cortical malformations may be able to be detected prior to the onset of seizures. Furthermore, whether upregulation of TSP and α2δ-1 reported here also occurs in adult injuries remains to be seen. Data from other in vitro models (Li et al., 2012; Liauw et al., 2008) suggest that GBP could remain efficacious, but whether GBP would be widely useful following adult brain injury has yet to be determined.

Our results clearly show that GBP decreases excitability and prevents many of the maladaptive changes that occur following FL, but the mechanism of these effects has yet to be determined. Based on our initial finding that TSP was increased in the FL cortex, we hypothesized that GBP would prevent FL-induced pathology via inhibition of TSP/α2δ-1 signaling. While our results are consistent with this hypothesis, they do not rule out that GBP has other non-specific effects. GBP has been shown to have effects on calcium currents via its actions on α2δ-1 trafficking (Hendrich et al., 2008; Hoppa et al., 2012) and to have α2δ-1 independent actions on ion channels (Liu et al., 2006) and ligand-gated NMDA and $GABA_B$ receptors (Kim et al., 2009; Ng et al., 2001; Lanneau et al., 2001). These effects may play a role in the protective properties of GBP in the FL model. We did perform parallel experiments using phenobarbital, a widely used anti-convulsant that has no known effect on TSP/α2δ-1 signaling. Phenobarbital treatment did not replicate GBP-induced attenuation of hyperexcitability. This result is consistent with the hypothesis that GBP's mechanism of action in the FL cortex is not due to its anticonvulsive properties. Future studies will more directly examine whether the effects of GBP reported here are due to interruption of TSP/α2δ-1 signaling. Although the mechanism for these effects remains uncertain, changes in TSP/α2δ-1-driven excitatory synaptogenesis have been suggested to mediate the therapeutic effects of GBP in several injury models (Li et al., 2012; Lo et al., 2011) and may play a role in the protective effects of GBP in the FL cortex.

Throughout our studies, we have assumed that astrocytes are the source of TSPs in the FL brain. Gene expression profiling in different brain cell types has shown that mRNAs for TSPs are mostly enriched in glia, in particular by postnatal astrocytes (Eroglu et al., 2009). TSP immunostaining was generally seen isotopically with GFAP positive reactive astrocytes and in the area of lesion. This is consistent with the hypothesis that astrocytes are the source of TSP following lesion. Interestingly, treatment with GBP decreased astrocyte reactivity at later developmental time points, as assayed by GFAP immunolabeling. Similar results of GBP treatment were also seen following pilocarpine administration (Rossi et al., 2013) and partial cortical isolation (Li et al., 2012). If astrocytes themselves are the source of TSP, this would suggest a feed-forward pathway leading to prolonged and/or additional astrocyte reactivity. This pathway may depend on increased neuronal glutamate release, as exposure to glutamate has been shown to increase GFAP expression (Floyd et al., 2004; Lievens et al., 2000; Inglis and Semba, 1997). Future studies will be aimed at determining whether astrocytes are the source of TSPs following cortical insult. TSPs are also known to be secreted by endothelial, neuronal and macrophage cells, including microglia (Risher and Eroglu, 2012; Liauw et al., 2008; Lin et al., 2003; Chamak et al., 1994). Furthermore, breach of the blood brain barrier may allow TSP into the neuropil from the circulatory system (Adams and Lawler, 2004). We plan to investigate this in future studies as well as the mechanism by which GBP decreases GFAP

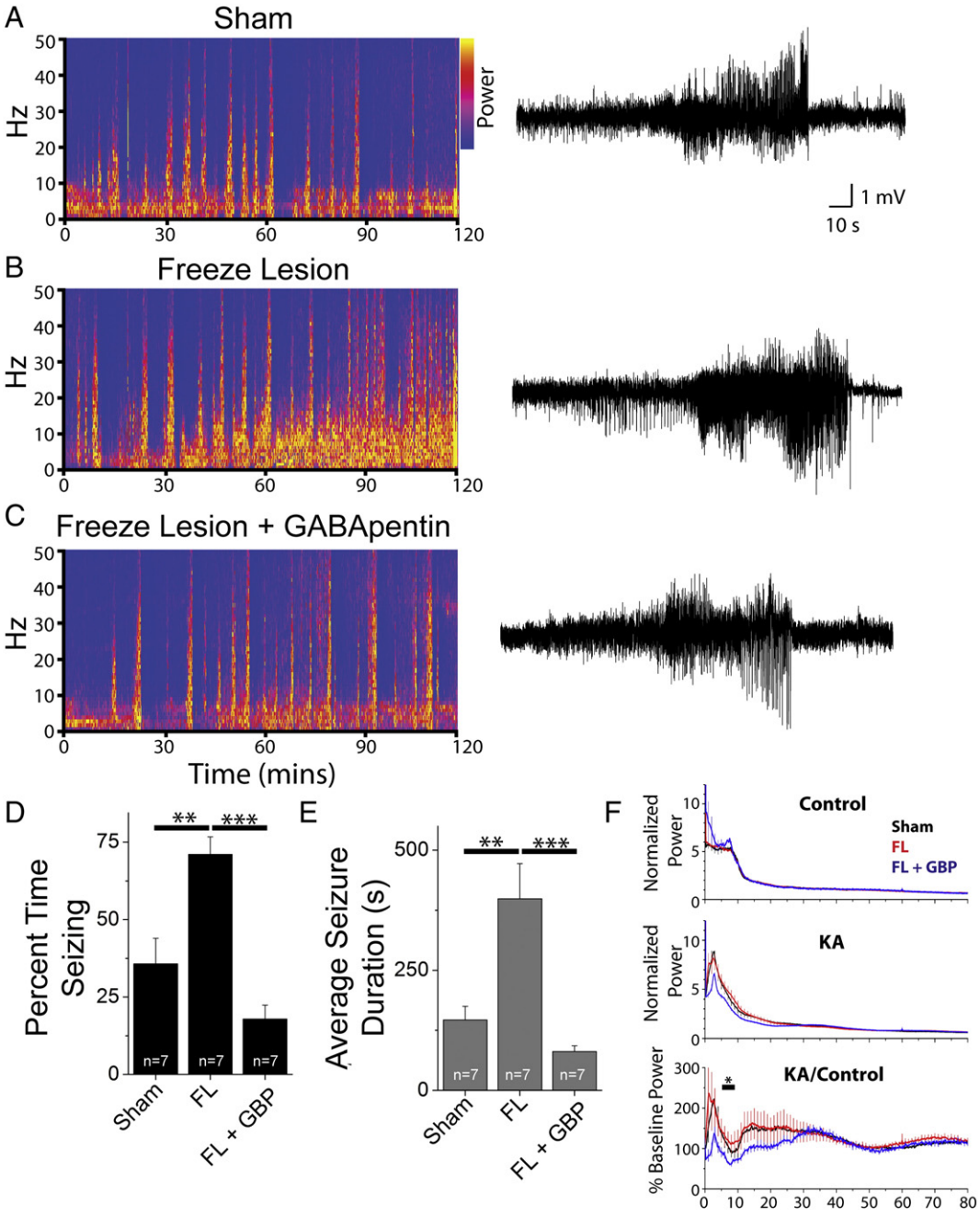

Fig. 7. Gabapentin treatment decreases in vivo kainic acid-induced seizure activity Representative power spectrum from 2 hour EEG recording of (A) sham injured, (B) FL and (C) GBP treated FL animals following acute kainic acid injection. (D) Percent time seizing and (E) average seizure duration, $^{**}p < 0.01$, $^{***}p < 0.001$. (F) Spectral analysis of EEG from sham (black), FL (red) and GBP treated FL animals (blue). Top, pre-kainic acid EEG, middle, kainic acid EEG, bottom, % baseline power normalized to pre-kainic acid EEG, $^{*}p < 0.05$.

immunolabeling. These findings will be critical to determining if and how these finding might be translated into a useful clinical approach.

In summary, the current study demonstrates that a GBP treatment regimen administered in the week following FL can decrease FL-induced epileptiform activity. These results suggest that GBP administered in a key therapeutic time window may have anti-epileptogenic properties following neonatal injury. We are especially interested in exploring the use of GBP in diseases that are 1) characterized by reactive astrocytosis and 2) occur in the young brain, during the normal developmental expression of TSP (Eroglu et al., 2009). Elucidating the therapeutic potential of targeting maladaptive TSP signaling is especially exciting as growing evidence links thrombospondins (TSPs) to brain pathology associated with a variety of insults (Rossi et al., 2013; Li et al., 2012; Liauw et al., 2008; Lin et al., 2003). Future studies addressing the mechanism of action responsible for the observed protective effects of GBP will shed new light on how hyperexcitable networks are formed following neonatal FL and will help to optimize treatment strategies for epilepsies associated with developmental cortical malformations.

Acknowledgments

This work was supported by the National Institute of Neurological Disease and Stroke (R01-NS076885, CD; R01-NS073574, JM), Epilepsy Foundation (CD), National Institute of Mental Health (R01-MH099554) (YY), and Tufts Center for Neuroscience Research (P30 NS047243). We thank the Imaging core facilities at Tufts University, which is supported by the Tufts Center for Neuroscience

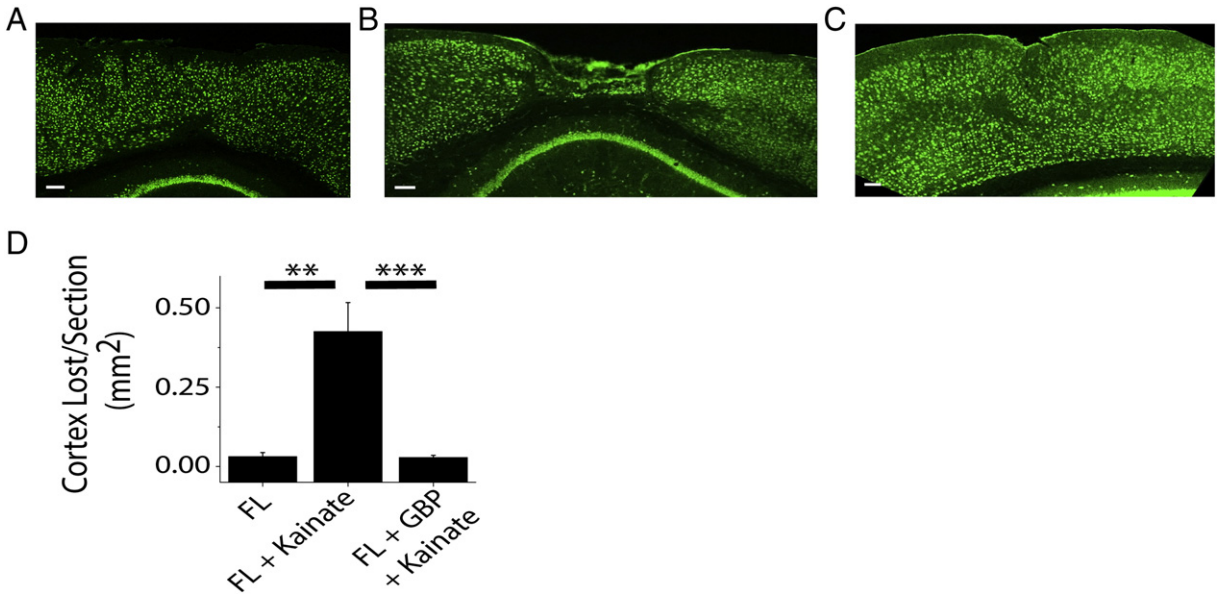

Fig. 8. Gabapentin treatment protects against cortical tissue loss following acute kainic acid injection. Representative images of NeuN staining of cortex of (A) FL animal treated with vehicle, (B) FL animal treated with kainic acid and (C) GBP treated FL animal treated with kainic acid. Scale bar = 100 μm. (D) Average cortical tissue lost per section, $^{**}p < 0.01$, $^{***}p < 0.001$.

Research. We also thank Dr. Sally McIver for help with the manuscript preparation and Dr. Maribel Rios and Dr. Moritz Armbruster for helpful discussions about TSP/α2δ-1 signaling.

References

Adams, J.C., Lawler, J., 2004. The thrombospondins. Int. J. Biochem. Cell Biol. 36, 961–968.

Asch, A.S., Leung, L.L., Shapiro, J., Nachman, R.L., 1986. Human brain glial cells synthesize thrombospondin. Proc. Natl. Acad. Sci. U. S. A. 83, 2904–2908.

Bordey, A., Lyons, S.A., Hablitz, J.J., Sontheimer, H., 2001. Electrophysiological characteristics of reactive astrocytes in experimental cortical dysplasia. J. Neurophysiol. 85, 1719–1731.

Brill, J., Huguenard, J.R., 2010. Enhanced infragranular and supragranular synaptic input onto layer 5 pyramidal neurons in a rat model of cortical dysplasia. Cereb. Cortex 20, 2926–2938.

Campbell, S.L., Hablitz, J.J., 2008. Decreased glutamate transport enhances excitability in a rat model of cortical dysplasia. Neurobiol. Dis. 32, 254–261.

Castro, O.W., Santos, V.R., Pun, R.Y., McKlveen, J.M., Batie, M., Holland, K.D., et al., 2012. Impact of corticosterone treatment on spontaneous seizure frequency and epileptiform activity in mice with chronic epilepsy. PLoS ONE 7, e46044.

Chamak, B., Morandi, V., Mallat, M., 1994. Brain macrophages stimulate neurite growth and regeneration by secreting thrombospondin. J. Neurosci. Res. 38, 221–233.

Christopherson, K.S., Ullian, E.M., Stokes, C.C., Mullowney, C.E., Hell, J.W., Agah, A., et al., 2005. Thrombospondins are astrocyte-secreted proteins that promote CNS synaptogenesis. Cell 120, 421–433.

Defazio, R.A., Hablitz, J.J., 2000. Alterations in NMDA receptors in a rat model of cortical dysplasia. J. Neurophysiol. 83, 315–321.

Dulla, C., Tani, H., Okumoto, S., Frommer, W.B., Reimer, R.J., Huguenard, J.R., 2008. Imaging of glutamate in brain slices using FRET sensors. J. Neurosci. Methods 168, 306–319.

Dulla, C.G., Tani, H., Brill, J., Reimer, R.J., Huguenard, J.R., 2012. Glutamate biosensor imaging reveals dysregulation of glutamatergic pathways in a model of developmental cortical malformation. Neurobiol. Dis. 49C, 232–246.

Eroglu, C., 2009. The role of astrocyte-secreted matricellular proteins in central nervous system development and function. J. Cell Commun. Signal. 3, 167–176.

Eroglu, C., Allen, N.J., Susman, M.W., O'Rourke, N.A., Park, C.Y., Ozkan, E., et al., 2009. Gabapentin receptor alpha2delta-1 is a neuronal thrombospondin receptor responsible for excitatory CNS synaptogenesis. Cell 139, 380–392.

Floyd, C.L., Rzigalinski, B.A., Sitterding, H.A., Willoughby, K.A., Ellis, E.F., 2004. Antagonism of group I metabotropic glutamate receptors and PLC attenuates increases in inositol trisphosphate and reduces reactive gliosis in strain-injured astrocytes. J. Neurotrauma 21, 205–216.

Gee, N.S., Brown, J.P., Dissanayake, V.U., Offord, J., Thurlow, R., Woodruff, G.N., 1996. The novel anticonvulsant drug, gabapentin (Neurontin), binds to the alpha2delta subunit of a calcium channel. J. Biol. Chem. 271, 5768–5776.

Guerrini, R., Dobyns, W.B., 2014. Malformations of cortical development: clinical features and genetic causes. Lancet Neurol. 13, 710–726.

Hagemann, G., Kluska, M.M., Redecker, C., Luhmann, H.J., Witte, O.W., 2003. Distribution of glutamate receptor subunits in experimentally induced cortical malformations. Neuroscience 117, 991–1002.

Hendrich, J., Van Minh, A.T., Heblich, F., Nieto-Rostro, M., Watschinger, K., Striessnig, J., et al., 2008. Pharmacological disruption of calcium channel trafficking by the alpha2delta ligand gabapentin. Proc. Natl. Acad. Sci. U. S. A. 105, 3628–3633.

Hoppa, M.B., Lana, B., Margas, W., Dolphin, A.C., Ryan, T.A., 2012. alpha2delta expression sets presynaptic calcium channel abundance and release probability. Nature 486, 122–125.

Inglis, W.L., Semba, K., 1997. Discriminable excitotoxic effects of ibotenic acid, AMPA, NMDA and quinolinic acid in the rat laterodorsal tegmental nucleus. Brain Res. 755, 17–27.

Jacobs, K.M., Prince, D.A., 2005. Excitatory and inhibitory postsynaptic currents in a rat model of epileptogenic microgyria. J. Neurophysiol. 93, 687–696.

Jacobs, K.M., Gutnick, M.J., Prince, D.A., 1996. Hyperexcitability in a model of cortical maldevelopment. Cereb. Cortex 6, 514–523.

Jacobs, K.M., Hwang, B.J., Prince, D.A., 1999. Focal epileptogenesis in a rat model of polymicrogyria. J. Neurophysiol. 81, 159–173.

Kamada, T., Sun, W., Takase, K., Shigeto, H., Suzuki, S.O., Ohyagi, Y., et al., 2013. Spontaneous seizures in a rat model of multiple prenatal freeze lesioning. Epilepsy Res. 105, 280–291.

Kellinghaus, C., Moddel, G., Shigeto, H., Ying, Z., Jacobsson, B., Gonzalez-Martinez, J., et al., 2007. Dissociation between in vitro and in vivo epileptogenicity in a rat model of cortical dysplasia. Epileptic Disord. 9, 11–19.

Kim, Y.S., Chang, H.K., Lee, J.W., Sung, Y.H., Kim, S.E., Shin, M.S., et al., 2009. Protective effect of gabapentin on N-methyl-D-aspartate-induced excitotoxicity in rat hippocampal CA1 neurons. J. Pharmacol. Sci. 109, 144–147.

Klaassen, A., Glykys, J., Maguire, J., Labarca, C., Mody, I., Boulter, J., 2006. Seizures and enhanced cortical GABAergic inhibition in two mouse models of human autosomal dominant nocturnal frontal lobe epilepsy. Proc. Natl. Acad. Sci. U. S. A. 103, 19152–19157.

Lanneau, C., Green, A., Hirst, W.D., Wise, A., Brown, J.T., Donnier, E., et al., 2001. Gabapentin is not a GABAB receptor agonist. Neuropharmacology 41, 965–975.

Lee, V., Maguire, J., 2013. Impact of inhibitory constraint of interneurons on neuronal excitability. J. Neurophysiol. 110, 2520–2535.

Leventer, R.J., Jansen, A., Pilz, D.T., Stoodley, N., Marini, C., Dubeau, F., et al., 2010. Clinical and imaging heterogeneity of polymicrogyria: a study of 328 patients. Brain 133, 1415–1427.

Li, H., Graber, K.D., Jin, S., McDonald, W., Barres, B.A., Prince, D.A., 2012. Gabapentin decreases epileptiform discharges in a chronic model of neocortical trauma. Neurobiol. Dis. 48, 429–438.

Liauw, J., Hoang, S., Choi, M., Eroglu, C., Choi, M., Sun, G.H., et al., 2008. Thrombospondins 1 and 2 are necessary for synaptic plasticity and functional recovery after stroke. J. Cereb. Blood Flow Metab. 28, 1722–1732.

Lievens, J.C., Bernal, F., Forni, C., Mahy, N., Kerkerian-Le, G.L., 2000. Characterization of striatal lesions produced by glutamate uptake alteration: cell death, reactive gliosis, and changes in GLT1 and GADD45 mRNA expression. Glia 29, 222–232.

Lin, T.N., Kim, G.M., Chen, J.J., Cheung, W.M., He, Y.Y., Hsu, C.Y., 2003. Differential regulation of thrombospondin-1 and thrombospondin-2 after focal cerebral ischemia/reperfusion. Stroke 34, 177–186.

Liu, Y., Qin, N., Reitz, T., Wang, Y., Flores, C.M., 2006. Inhibition of the rat brain sodium channel Nav1.2 after prolonged exposure to gabapentin. Epilepsy Res. 70, 263–268.

Lo, F.S., Zhao, S., Erzurumlu, R.S., 2011. Astrocytes promote peripheral nerve injury-induced reactive synaptogenesis in the neonatal CNS. J. Neurophysiol. 106, 2876–2887.

Luhmann, H.J., Karpuk, N., Qu, M., Zilles, K., 1998a. Characterization of neuronal migration disorders in neocortical structures. II. Intracellular in vitro recordings. J. Neurophysiol. 80, 92–102.

Luhmann, H.J., Raabe, K., Qu, M., Zilles, K., 1998b. Characterization of neuronal migration disorders in neocortical structures: extracellular in vitro recordings. Eur. J. Neurosci. 10, 3085–3094.
Macdonald, R.L., Barker, J.L., 1978. Different actions of anticonvulsant and anesthetic barbiturates revealed by use of cultured mammalian neurons. Science 200, 775–777.
Maguire, J., Mody, I., 2009. Steroid hormone fluctuations and GABA(A)R plasticity. Psychoneuroendocrinology 34 (Suppl. 1), S84–S90.
Maguire, J.L., Stell, B.M., Rafizadeh, M., Mody, I., 2005. Ovarian cycle-linked changes in GABA(A) receptors mediating tonic inhibition alter seizure susceptibility and anxiety. Nat. Neurosci. 8, 797–804.
Ng, G.Y., Bertrand, S., Sullivan, R., Ethier, N., Wang, J., Yergey, J., et al., 2001. Gamma-aminobutyric acid type B receptors with specific heterodimer composition and post-synaptic actions in hippocampal neurons are targets of anticonvulsant gabapentin action. Mol. Pharmacol. 59, 144–152.
Ning, M., Sarracino, D.A., Kho, A.T., Guo, S., Lee, S.R., Krastins, B., et al., 2011. Proteomic temporal profile of human brain endothelium after oxidative stress. Stroke 42, 37–43.
Risher, W.C., Eroglu, C., 2012. Thrombospondins as key regulators of synaptogenesis in the central nervous system. Matrix Biol. 31, 170–177.
Rossi, A.R., Angelo, M.F., Villarreal, A., Lukin, J., Ramos, A.J., 2013. Gabapentin administration reduces reactive gliosis and neurodegeneration after pilocarpine-induced status epilepticus. PLoS ONE 8, e78516.
Scantlebury, M.H., Ouellet, P.L., Psarropoulou, C., Carmant, L., 2004. Freeze lesion-induced focal cortical dysplasia predisposes to atypical hyperthermic seizures in the immature rat. Epilepsia 45, 592–600.
Sills, G.J., 2006. The mechanisms of action of gabapentin and pregabalin. Curr. Opin. Pharmacol. 6, 108–113.
Takano, T., Sokoda, T., Akahori, S., Sakaue, Y., Sawai, C., Takeuchi, Y., et al., 2006. Enhanced capacity of epilepsy in brain malformation produced during early development. Pediatr. Neurol. 35, 38–41.
Ullian, E.M., Sapperstein, S.K., Christopherson, K.S., Barres, B.A., 2001. Control of synapse number by glia. Science 291, 657–661.
Ullian, E.M., Barkis, W.B., Chen, S., Diamond, J.S., Barres, B.A., 2004a. Invulnerability of retinal ganglion cells to NMDA excitotoxicity. Mol. Cell. Neurosci. 26, 544–557.
Ullian, E.M., Christopherson, K.S., Barres, B.A., 2004b. Role for glia in synaptogenesis. Glia 47, 209–216.
Wang, T., Kumada, T., Morishima, T., Iwata, S., Kaneko, T., Yanagawa, Y., et al., 2012. Accumulation of GABAergic neurons, causing a focal ambient GABA gradient, and down-regulation of KCC2 are induced during microgyrus formation in a mouse model of polymicrogyria. Cereb. Cortex 24, 1088–1101.
Zhou, H.J., Zhang, H.N., Tang, T., Zhong, J.H., Qi, Y., Luo, J.K., et al., 2010. Alteration of thrombospondin-1 and -2 in rat brains following experimental intracerebral hemorrhage. Laboratory investigation. J. Neurosurg. 113, 820–825.
Zilles, K., Qu, M., Schleicher, A., Luhmann, H.J., 1998. Characterization of neuronal migration disorders in neocortical structures: quantitative receptor autoradiography of ionotropic glutamate, GABA(A) and GABA(B) receptors. Eur. J. Neurosci. 10, 3095–3106.
Zsombok, A., Jacobs, K.M., 2007. Postsynaptic currents prior to onset of epileptiform activity in rat microgyria. J. Neurophysiol. 98, 178–186.